

Dra. Laura Rodríguez Raurell
*Departament de Química Inorgànica i
Orgànica*

Dr. Ignacio Alfonso Rodríguez
IQAC-CSIC



Treball Final de Grau

**Supramolecular Au(I) systems with luminescent properties.
Aggregation studies.**

**Sistemes supramoleculars d'Au(I) amb propietats luminescents.
Estudis d'agregació.**

Jaume Sonet Ventosa

June 2018



UNIVERSITAT DE
BARCELONA

B:KC Barcelona
Knowledge
Campus
Campus d'Excel·lència Internacional

Aquesta obra esta subjecta a la llicència de:
Reconeixement–NoComercial–SenseObraDerivada



<http://creativecommons.org/licenses/by-nc-nd/3.0/es/>

La veritat requereix rigor. La mentida, imaginació.

Jorge Wagensberg

L'agraïment en els moments de cloure projectes i etapes és una necessitat vivíssima, gairebé vital. El sentiment que m'agradaria expressar té la voluntat d'estendre's cap a totes les persones que m'heu fet costat, m'heu ensenyat i m'heu fet créixer durant aquests mesos de TFG i aquests anys de carrera. A tots i totes vosaltres desitjo que us arribi aquest missatge senzill i afectuós:

Gràcies per ser-hi.

REPORT

CONTENTS

1. SUMMARY	3
2. RESUM	5
3. INTRODUCTION	7
3.1. Background	7
3.2. Starting point of the reported research	8
4. OBJECTIVES	10
5. EXPERIMENTAL SECTION	11
5.1. Materials, general procedures and physical measurements	11
5.2. Syntheses	12
5.2.1. Synthesis of pyPEG	12
5.2.2. Synthesis of [AuCl(tht)]	13
5.2.3. Synthesis of [AuCl(pyPEG)]	13
5.2.4. Synthesis of [Au(EA)(pyPEG)]	14
5.2.5. Synthesis of [Au(PC7)(pyPEG)]	15
5.3. UV-Vis absorption and emission measurements	16
5.4. Optical microscopy	17
6. RESULTS AND DISCUSSION	18
6.1. Synthesis and characterization	18
6.2. Photophysical characterization of [Au(PC7)(pyPEG)] solutions	24
6.3. Aggregation studies of [Au(PC7)(pyPEG)] solutions	25
6.3.1. UV-Vis absorption and emission measurements	25
6.3.2. NMR spectroscopy	30
6.3.3. SAXS	30
6.3.4. Optical microscopy	32
7. CONCLUSIONS	34
8. REFERENCES AND NOTES	35
9. ACRONYMS	37

1. SUMMARY

Gold(I) organometallic compounds display electronic properties that make them suitable candidates for constituting supramolecular aggregates and presenting absorption and emission of ultraviolet-visible radiation. The present research project describes the synthesis of two gold(I) organometallic compounds where the metallic centre is coordinated to a pyridine-type ligand bonded to a polyethylene glycol (PEG) structure, as well as alkynyl ligands bonded to chromophore groups (aniline or coumarin).

Aggregation of one of the synthesized compounds dissolved in acetonitrile and acetonitrile / water mixtures in variable proportions has been studied. By means of ultraviolet-visible absorption and emission measurements, some indicators of aggregation have been found. In addition, in this project there is a study of how aggregation is affected by the solute concentration and the relative content of water in the solvent.

Finally, SAXS (small angle X-ray scattering) experiments and optical microscopy observations have been performed to obtain more experimental evidences of the presence of supramolecular aggregates in the solutions from the studied compound. The scope of the research included to analyse their sizes, shapes and aggregation morphologies.

Keywords: Aggregation, gold(I), luminescence, supramolecular chemistry, pyridine ligand, PEG, alkynyl ligand, coumarin.

2. RESUM

Els compostos organometàl·lics d'or(I) tenen propietats electròniques que els fan ser bons candidats a formar agregats supramoleculars i a presentar absorció i emissió de radiació ultraviolat-visible. En aquest Treball Final de Grau s'han sintetitzat dos compostos organometàl·lics d'or(I) en els quals el centre metàl·lic està coordinat a un lligand de tipus piridina unit a una estructura de tipus polietilenglicol (PEG), així com també a lligands alquinil units a grups cromòfors (anilina o cumarina).

S'ha estudiat l'agregació d'un dels compostos sintetitzats dissolt en acetonitril i en sistemes acetonitril / aigua en proporcions variables. Mitjançant mesures d'absorció i emissió ultraviolat-visible s'han trobat diversos indicadors que demostren el procés d'agregació. A més, s'ha estudiat la influència de la concentració de solut i de la proporció d'aigua del dissolvent en l'agregació.

Per últim, s'han dut a terme experiments de SAXS (dispersió de raigs X a angles petits) i s'ha emprat microscòpia òptica per tal d'obtenir altres evidències experimentals de la presència d'agregats supramoleculars en solucions del compost estudiat, analitzant les seves mides, formes i morfologies d'agregació.

Paraules clau: Agregació, or(I), luminescència, química supramolecular, lligand piridina, PEG, lligand alquinil, cumarina.

3. INTRODUCTION

3.1. BACKGROUND

Gold is well-known for having an outstanding interest, not only because of the brightness of metallic gold and its alloys but also due to its inertness and other noble properties. Moreover, organometallic gold compounds have gathered a remarkable attention in the last decades. Particularly, Au(I) has a closed-shell electronic configuration that enables it to establish metal···metal interactions, known as *aurophilicity* ^[1,2]. This type of non-covalent interactions is associated to an Au···Au distance of *ca.* 3.0–3.5 Å, shorter than the sum of two van der Waals radii of Au(I), and a bond energy of 5–10 kcal/mol, comparable to hydrogen bonding ^[3]. *Aurophilic* interactions can lead to the formation of supramolecular aggregates and self-assembled structures, especially when combined with other interactions such as hydrogen bonding, π - π stacking interactions, hydrophobic effects or van der Waals forces.

Besides the stabilizing effect, the presence of Au(I) centres in molecules can decrease the energy gap between their HOMO (highest occupied molecular orbital) and LUMO (lowest unoccupied molecular orbital), resulting in higher chances of manifesting photophysical properties. As the synthesis of efficient luminescent materials is a research branch currently in expansion, organometallic gold compounds are a field to develop. There is a wide range of applications in which Au(I) luminescent complexes are used, *e.g.* molecular recognition ^[4], optical sensors ^[5], antitumor activity ^[6] and molecular machines ^[7].

Aggregation in Au(I) organometallic compounds can be modulated by several factors and one of the key elements is the solvent. In 2013, in the research group where this project has been performed there was the discovery that some Au(I) complexes form luminescent hydrogels ^[8]. In fact, supramolecular gels, also known as low molecular mass gelators, have been actively investigated in the last three decades and there has been the incorporation of metal complexes in organic-based gelators, giving rise to supramolecular metallo-gelators. Some metallo-organogels –gelator molecules with metal centres which immobilize organic solvents– and metallohydrogels –the ones that enclose water molecules– are constituted by Au(I) atoms

[9]. Some studies in the research group [10-14] show that aggregation in Au(I) supramolecular structures that form gels has a strong dependence on the solvent in which they are dissolved.

The diversity of metal-ligand coordination can generate different geometries, topologies and interactions. Therefore, as it influences the process of aggregation and the substance properties, it offers a horizon of possibilities in terms of research. Thus, aggregation can be enhanced by making a rational molecular design of the compounds. In this sense, PEG (polyethylene glycol) structures are interesting moieties to incorporate in complexes due to their facility to establish hydrogen bondings [15,16]. Besides, alkynyl units connected to π -insaturated organic groups have the appropriate topology and electronic properties to make them suitable to set up supramolecular interactions in organometallic gold complexes [17,18]. Research in gold(I) containing alkynyl moieties has increased during the last 20 years and nowadays it has led to applications in different fields, including catalysis, biomedical sciences and material science [19]. The research group where this work has been performed has studied a large number of Au(I) organometallic compounds with alkynyl groups [10-14,20,21].

Moreover, some of the mentioned compounds incorporate alkynyl-coumarin moieties [11,20,21]; coumarin is an organic structure characterized by having a light emission that can be tunable by changing its substituents and solvent [22,23], which is a valuable property with a wide range of applications.

Pyridine-type ligands, which have the capacity to coordinate transition metals and photophysical properties since they can act as emitters themselves, are also interesting for their versatility. Nevertheless, although the existence of Au–N dative covalent bonds has been proved in pyridines [24], organometallic gold complexes with pyridine-type ligands are limited and there are few reports on the luminescent properties of them [25]. Consequently, there is a hidden potential in this type of compounds.

3.2. STARTING POINT OF THE REPORTED RESEARCH

All the mentioned details are the key elements of the work reported herein. The starting point is a molecule which appears in two articles from Aliprandi et al. [26] and Carrara et al. [27], where it is part of a synthetic route to obtain a ligand that coordinates Pt(II) compounds. This molecule, called pyPEG from now on, can act as a pyridine-type ligand and has a PEG tail,

features that make it an interesting structure to generate luminescent supramolecular aggregates. Two Au(I) complexes with the pyPEG molecule and an alkynyl ligand bonded to a π -insaturated organic group have been designed to form supramolecular structures with photophysical properties; their structure can be seen in figure 1. In the case of [Au(EA)(pyPEG)], EA means 4-ethynylaniline, whereas in [Au(PC7)(pyPEG)] PC7 is the abbreviation of 7-propargylcoumarin.

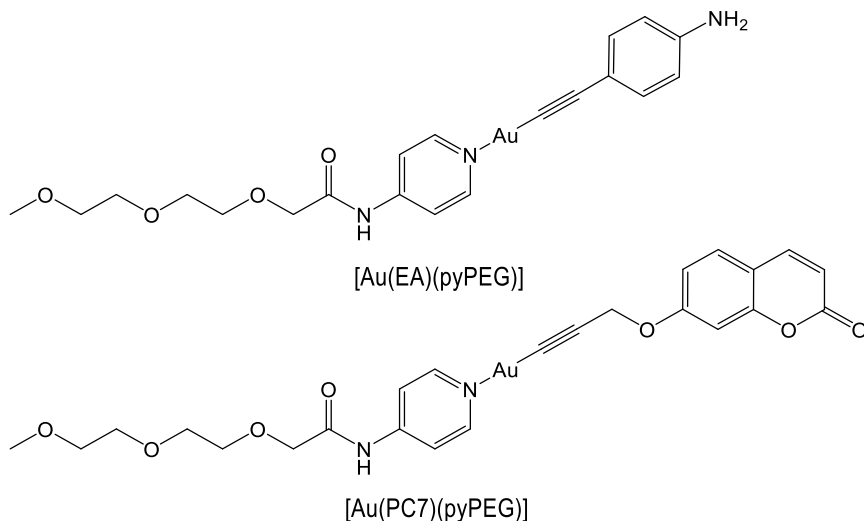


Figure 1. Molecules that have been designed and synthesized in this work and their abbreviations.

Furthermore, apart from the synthesis and characterization of both compounds, in this report there is a study of aggregation in [Au(PC7)(pyPEG)] solutions taking advantage of the photophysical properties of the compound.

4. OBJECTIVES

The first objective of this project is to synthesize two Au(I) organometallic complexes containing a pyPEG ligand and an alkynyl ligand bonded to a π -unsaturated organic group (EA and PC7). In order to prove their successful synthesis, the two compounds will be characterized by infrared (IR) spectra, proton Nuclear Magnetic Resonance ($^1\text{H-NMR}$) and Electrospray Ionization Mass Spectrometry (ESI-MS).

Secondly, it is aimed to examine the supramolecular aggregation of $[\text{Au}(\text{PC7})(\text{pyPEG})]$ in solution with ultraviolet-visible (UV-Vis) absorption and emission measurements in different solvent systems, as well as $^1\text{H-NMR}$ spectra. These experiments pursue to provide evidence of the aggregation phenomenon present in the solutions, to know which moieties of the molecule are involved in it and also to study the influence of the solute concentration and the composition of the solvent in aggregation.

Finally, the objective to provide experimental evidence of supramolecular aggregation of $[\text{Au}(\text{PC7})(\text{pyPEG})]$ in solution will be complemented by SAXS (Small Angle X-ray Scattering) measurements and optical microscopy. These techniques are aimed to analyse the size, shape and morphology of the aggregates.

5. EXPERIMENTAL SECTION

5.1. MATERIALS, GENERAL PROCEDURES AND PHYSICAL MEASUREMENTS

Materials and general procedures

All reactions and manipulations were carried out in high-purity N₂ by using standard Schlenk techniques. Used dry solvents (dichloromethane, hexane) were taken from a Solvent Purification System (Innovative Technologies). Milli-Q water, MeOH p.a. (Scharlau), EtOH p.a. (Scharlau), AcOEt p.a. (Aldrich), DMSO p.a. (Aldrich), ACN p.a. (Scharlau) and THF p.a. (Scharlau) were purged 30 min under N₂ flow prior to use. Reagents and auxiliary substances used were tetrachloroauric acid (Aldrich), tetrahydrothiophene (Merck), 4-aminopyridine (Aldrich), N,N'-dicyclohexylcarbodiimide (Aldrich), 2-[2-(2-methoxyethoxy)ethoxy]acetic acid (Aldrich), 4-ethynylaniline (Aldrich) and potassium hydroxide (Fisher Chemical), and were used as received. ¹H-NMR spectra were recorded in CDCl₃, DMSO-d₆ and ACN-d₃, which were purchased from Euriso-top. Literature methods were used to prepare pyPEG [26,27], [AuCl(tht)] [28] and [AuCl(pyPEG)] [29]. PC7 was previously synthesized by other researchers in the group, as reported [20].

Physical measurements

Infrared spectra were recorded on a FT-IR 520 Nicolet spectrophotometer. ¹H NMR spectra [δ (TMS) = 0.0 ppm] were obtained on a Varian Mercury 400 spectrometer. Positive-mode electrospray ionization mass spectrometry [ESI-MS(+)] spectra were recorded on a Fisons VG Quattro spectrometer. Absorption spectra were recorded on a Varian Cary 100 Bio UV spectrophotometer and emission spectra on Horiba-Jobin-Yvon SPEX Fluorolog 3.22 and Nanolog spectrofluorimeters. Optical microscopy images were acquired on a Leica ICC50 W microscope equipped with a Nikon DXM1200F digital camera.

SAXS (small angle X-ray scattering) experiments were performed at the NCD beamline at the Alba Synchrotron at 12.4 keV, with a sample/detector distance of 2.2 m. The data were collected on an ImXPad S1400 detector with a pixel size of 130.0 × 130.0 μm². Temperature of the samples was 20 °C in all cases, exposure time was 10 s and the *q*-axis calibration was obtained by measuring silver behenate. The low-resolution structure of the aggregates was reconstructed ab initio from the initial portions of the scattering patterns using the *DAMMIN*

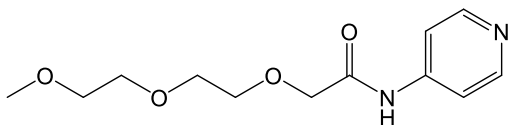
program [30]. Solutions of $1 \cdot 10^{-4}$ and $1 \cdot 10^{-5}$ M of compounds [AuCl(pyPEG)], [Au(EA)(pyPEG)] and [Au(PC7)(pyPEG)] were prepared in different ACN/H₂O mixtures (0%, 5%, 10%, 25%, 50%, 75% and 90% ACN).

TLC was carried out with aluminium pre-coated silica gel 0.2 mm plates. Column chromatography was performed using Fluka silica gel (60 Å).

5.2. SYNTHESSES

5.2.1. Synthesis of pyPEG

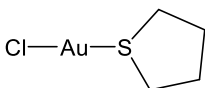
According to the literature procedure [26,27], 2-[2-(2-methoxyethoxy)ethoxy]acetic acid (5.724 g, 32.13 mmol) and 4-aminopyridine (2.005 g, 21.31 mmol) were dissolved in 100 mL of CHCl₃, then N,N'-dicyclohexylcarbodiimide (DCC) (6.590 g, 31.94 mmol) was added in consecutive little aliquots. During the addition, a white precipitate was formed. The solution was stirred for one hour at room temperature and then refluxed for four hours. After cooling down to room temperature, the solution was filtrated and the filtrate concentrated in vacuum. The resulting crude yellow oil was purified by column chromatography on silica gel using AcOEt to AcOEt/MeOH 9:1, monitoring the process with TLC till obtaining the pure product, which was a pale-yellow oil. Yield: 16% (0.860 g).



IR (KBr, cm⁻¹): 3427 (N-H), 3079 (C_{sp2}-H), 2923 (C_{sp3}-H), 1703 (C=O), 1594 (C=N), 1515 (C=C). ¹H NMR (CDCl₃, 400 MHz, ppm): δ 8.99 (br. s, 1H, N-H), 8.51 (d, J = 6.0 Hz, 2H, N_{py}-CH), 7.59 (d, J = 6.0 Hz, 2H, N_{py}-CH-CH), 4.11 (s, 2H, CO-CH₂), 3.78 – 3.58 (m, 8H, CH₃-O-CH₂-CH₂-O-CH₂-CH₂), 3.37 (s, 3H, -CH₃). ESI-MS(+): *m/z* 255.1347 ([M+H]⁺). Calculated M⁺ *m/z*: 254.1267, calculated [M+H]⁺ *m/z*: 255.1339 (M⁺ = C₁₂H₁₈N₂O₄⁺).

5.2.2. Synthesis of [AuCl(tht)]

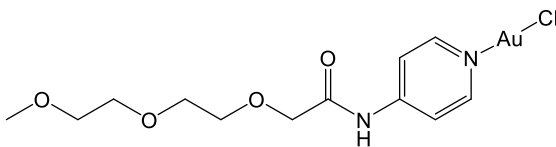
According to the literature procedure ^[28], HAuCl₄ (5.016 g, 14.8 mmol) was dissolved in a H₂O/EtOH solution (6.5 mL / 32 mL). Tht (1.80 mL, 20.4 mmol) was then added dropwise to the previous stirring solution. A yellow solid precipitated immediately. After 30 min of stirring, the precipitate was filtrated with a glass frit, washed with EtOH (3 × 10 mL) and dried under vacuum to obtain a white solid. Yield: 55% (2.625 g).



IR (KBr, cm⁻¹): 2916 (C_{sp3}-H), 1425 (C-C). ¹H NMR (CDCl₃, 400 MHz, ppm): δ 3.41 (br. d, J = 68 Hz, 2H, S-CH₂), 2.19 (br. d, J = 70 Hz, 2H, S-CH₂-CH₂).

5.2.3. Synthesis of [AuCl(pyPEG)]

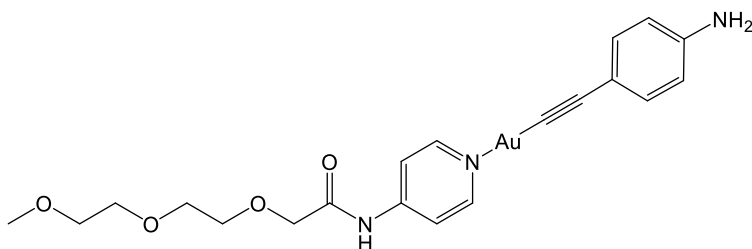
[AuCl(tht)] (0.1999 g, 0.6228 mmol) was dissolved in CH₂Cl₂ (5 mL) in a purged Schlenk covered by aluminium foil. pyPEG (0.1558 g, 0.6131 mmol) was dissolved in CH₂Cl₂ (5 mL). The pyPEG solution was added dropwise to the [AuCl(tht)] solution while stirring it, resulting in a white suspension. After 1 h of stirring, the reaction mixture was concentrated in vacuum, washed with hexane (5 mL) and left in a freezer for several hours. Later, the precipitate was filtrated through cannula and dried under vacuum, obtaining a white solid. Yield: 69% (0.1285 g).



IR (KBr, cm⁻¹): 3452 (N-H), 2885 (C_{sp3}-H), 1714 (C=O), 1622 (C=N), 1518 (C=C). ¹H NMR (CDCl₃, 400 MHz, ppm): δ 9.53 (br. s, 1H, N-H), 8.40 (d, J = 6.0 Hz, 2H, N_{py}-CH), 7.89 (d, J = 6.0 Hz, 2H, N_{py}-CH-CH), 4.15 (s, 2H, CO-CH₂), 3.78 – 3.60 (m, 8H, CH₃-O-CH₂-CH₂-O-CH₂-CH₂), 3.38 (s, 3H, -CH₃).

5.2.4. Synthesis of [Au(EA)(pyPEG)]

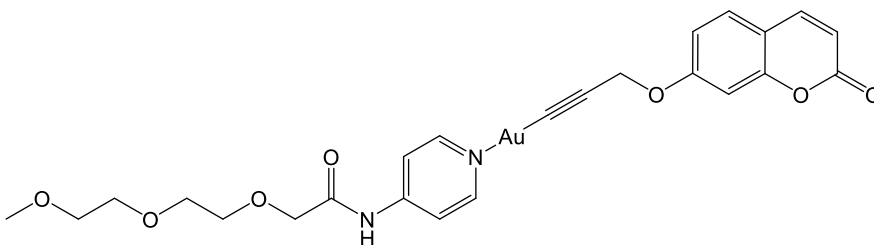
4-ethynylaniline (EA) (0.0148 g, 0.1263 mmol) was treated with KOH (0.0196 g, 0.3493 mmol) in MeOH (5 mL) under N₂ atmosphere. [AuCl(pyPEG)] (0.0596 g, 0.1225 mmol) was dissolved in CH₂Cl₂ (5 mL) and this solution was added dropwise to the previous one while stirring the mixture, leading to the formation of a reddish brown solid. After 1 h of stirring, the reaction mixture was concentrated under vacuum, washed with hexane (5 mL) and left in a freezer for several hours. Later, the precipitate was filtrated through cannula and dried under vacuum, obtaining a reddish brown solid. Yield: 59% (0.0410 g).



IR (KBr, cm⁻¹): 3436 (N-H), 2885 (C_{sp3}-H), 1996 (C≡C), 1715 (C=O), 1619 (C=N), 1511 (C=C). ¹H NMR (DMSO-d₆, 400 MHz, ppm): δ 9.99 (br. s, 1H, N-H), 8.40 (d, J = 6.0 Hz, 2H, N_{py}-CH), 7.60 (d, J = 6.0 Hz, 2H, N_{py}-CH-CH), 6.84 (d, J = 8.2 Hz, 2H, C≡C-C=CH), 6.37 (d, J = 8.2 Hz, 2H, C≡C-C=CH-CH), 4.98 (s, 2H, -NH₂), 4.09 (s, 2H, CO-CH₂), 3.65 – 3.20 (m, 11H, CH₃-O-CH₂-CH₂-O-CH₂-CH₂). ¹H NMR (ACN-d₃, 400 MHz, ppm): δ 9.03 (br. s, 1H, N-H), 8.45 (d, J = 6.0 Hz, 2H, N_{py}-CH), 7.61 (d, J = 6.0 Hz, 2H, N_{py}-CH-CH), 7.00 (d, J = 8.2 Hz, 2H, C≡C-C=CH), 6.49 (d, J = 8.2 Hz, 2H, C≡C-C=CH-CH), 4.07 (s, 2H, -NH₂), 4.05 (s, 2H, CO-CH₂), 3.75 – 3.48 (m, 8H, CH₃-O-CH₂-CH₂-O-CH₂-CH₂), 3.30 (s, 3H, -CH₃). ESI-MS(+): *m/z* 568.1496 ([M+H]⁺). Calculated M⁺ *m/z*: 567.1432, calculated [M+H]⁺ *m/z*: 568.1505 (M⁺: C₂₀H₂₄AuN₃O₄⁺).

5.2.5. Synthesis of [Au(PC7)(pyPEG)]

7-propargylcoumarin (PC7) (0.0184 g, 0.0919 mmol) was treated with KOH (0.0112 g, 0.1996 mmol) in MeOH (5 mL) under N₂ atmosphere. [AuCl(pyPEG)] (0.0447 g, 0.0918 mmol) was dissolved in CH₂Cl₂ (5 mL) and this solution was added dropwise to the previous one while stirring the mixture, leading to the formation of an ochre solid. After 1 h of stirring, the reaction mixture was concentrated under vacuum, washed with hexane (5 mL) and left in a freezer for several hours. Later, the precipitate was filtrated through cannula and dried under vacuum, obtaining a pale brown solid. Yield: 63% (0.0376 g).



IR (KBr, cm⁻¹): 3436 (N-H), 2920 (C_{sp3}-H), 2135 (C≡C), 1720 (C=O), 1612 (C=N), 1506 (C=C). ¹H NMR (DMSO-d₆, 400 MHz, ppm): δ 10.03 (br. s, 1H, N-H), 8.44 (d, J = 6.0 Hz, 2H, N_{py}-CH), 7.99 (d, J = 9.5 Hz, O-CO-CH-CH), 7.64 (d, J = 6.0 Hz, 2H, N_{py}-CH-CH), 7.61 (d, J = 8.5 Hz, 1H, O-CO-CH-CH-C-CH), 7.00 – 6.94 (m, 2H, CH₂-O-C-CH), 6.29 (d, J = 9.5 Hz, 1H, O-CO-CH), 4.81 (s, 2H, C≡C-CH₂), 4.13 (s, 2H, CO-CH₂), 3.68 – 3.42 (m, 8H, CH₃-O-CH₂-CH₂-O-CH₂-CH₂), 3.24 (s, 3H, -CH₃). ¹H NMR (ACN-d₃, 400 MHz, ppm): δ 9.04 (br. s, 1H, N-H), 8.44 (d, J = 6.0 Hz, 2H, N_{py}-CH), 7.77 (d, J = 9.5 Hz, O-CO-CH-CH), 7.60 (d, J = 6.0 Hz, 2H, N_{py}-CH-CH), 7.49 (d, J = 8.5 Hz, 1H, O-CO-CH-CH-C-CH), 6.96 – 6.91 (m, 2H, CH₂-O-C-CH), 6.17 (d, J = 9.5 Hz, 1H, O-CO-CH), 4.83 (s, 2H, C≡C-CH₂), 4.07 (s, 2H, CO-CH₂), 3.72 – 3.51 (m, 8H, CH₃-O-CH₂-CH₂-O-CH₂-CH₂), 3.29 (s, 3H, -CH₃). ESI-MS(+): *m/z* 651.1409 ([M+H]⁺). Calculated M⁺ *m/z*: 650.1327, calculated [M+H]⁺ *m/z*: 651.1400 (M⁺: C₂₄H₂₅AuN₂O₇⁺).

5.3. UV-VIS ABSORPTION AND EMISSION MEASUREMENTS

Aggregation studies in [Au(PC7)(pyPEG)] solutions varying its concentration

UV-Visible absorption and emission studies on [Au(PC7)(pyPEG)] were performed in DMSO/H₂O and in ACN/H₂O systems in a range of concentrations between *ca.* $5.0 \cdot 10^{-7}$ M and *ca.* $1.0 \cdot 10^{-4}$ M. Studies in a constant solvent with variation of concentration were performed as follows: solution I (*ca.* $5.0 \cdot 10^{-4}$ M) was prepared by weighing the adequate amount of [Au(PC7)(pyPEG)] and dissolving it, solutions II-IX were prepared according to the pattern in figure 2 using micropipette additions and all the spectra were recorded in a lapse of 2-3 hours introducing the solutions in a 10 mm path length prism-shaped quartz cell. DMSO 50% / H₂O 50%, ACN 100% and ACN 75% / H₂O 25% are the solvent systems with which the studies were carried out.

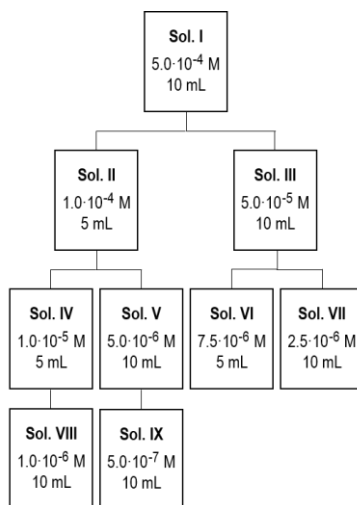


Figure 2. Dilution pattern used in the aggregation studies with variation of concentration.

Aggregation studies in [Au(PC7)(pyPEG)] solutions varying the solvent composition

Studies varying the relative amounts of ACN and H₂O in a ACN/H₂O solvent system were performed in concentrations of *ca.* $1.0 \cdot 10^{-4}$ M and *ca.* $1.0 \cdot 10^{-5}$ M, preparing previously a precursor $5.0 \cdot 10^{-4}$ M solution by weighing the adequate amount of [Au(PC7)(pyPEG)] and dissolving it in ACN. The solvent composition, solute concentration and preparation procedure of each sample are collected in table 1.

Sample	% H ₂ O	<i>ca.</i> c [M]	V _{precursor} [mL]	V _{ACN} [mL]	V _{H₂O} [mL]
1	0	$1.0 \cdot 10^{-4}$	1.00	4.00	0.00
2	5	$1.0 \cdot 10^{-4}$	1.00	3.75	0.25
3	10	$1.0 \cdot 10^{-4}$	1.00	3.50	0.50
4	15	$1.0 \cdot 10^{-4}$	1.00	3.25	0.75
5	20	$1.0 \cdot 10^{-4}$	1.00	3.00	1.00
6	25	$1.0 \cdot 10^{-4}$	1.00	2.75	1.25

7	0	$1.0 \cdot 10^{-5}$	0.10	4.90	0.00
8	5	$1.0 \cdot 10^{-5}$	0.10	4.65	0.25
9	10	$1.0 \cdot 10^{-5}$	0.10	4.40	0.50
10	15	$1.0 \cdot 10^{-5}$	0.10	4.15	0.75
11	20	$1.0 \cdot 10^{-5}$	0.10	3.90	1.00
12	25	$1.0 \cdot 10^{-5}$	0.10	3.65	1.25

Table 1. Solvent composition, solute ca. concentration and components of the samples used in the aggregation studies of [Au(PC7)(pyPEG)] in ACN/H₂O varying the solvent proportions.

5.4. OPTICAL MICROSCOPY

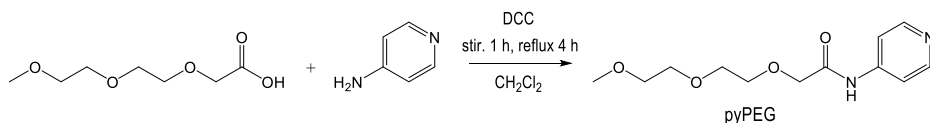
The solutions used in the aggregation studies detailed in the previous paragraphs were also treated to observe them with an optical microscope. The preparation of samples was done as follows: three drops of each sample were placed on a microscope slide and evaporated till dryness spontaneously, waiting 48 h with no application of heat. Observations were made using conventional visible light and polarized visible light.

6. RESULTS AND DISCUSSION

6.1. SYNTHESIS AND CHARACTERIZATION

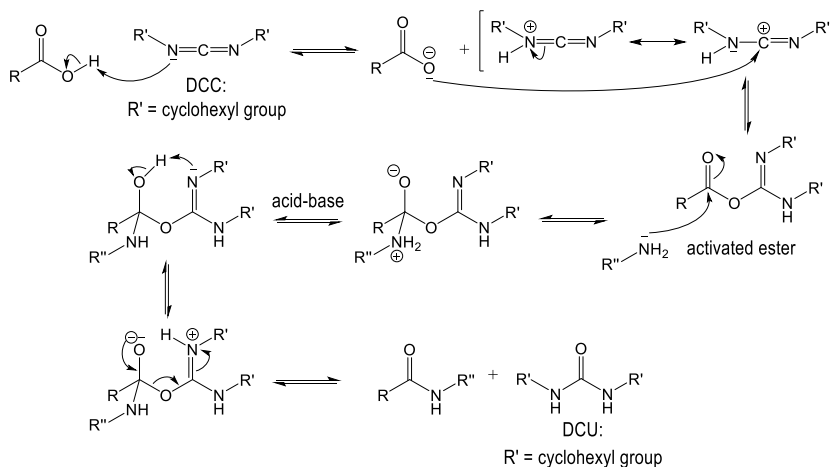
Synthesis of pyPEG

N-(4-pyridyl)-2-[2-(2-methoxyethoxy)ethoxy]acetic acid amide (abbreviated as pyPEG) was successfully synthesized using the literature method, summarized in scheme 1.



Scheme 1. Synthesis of pyPEG.

This reaction is a nucleophilic acyl substitution that affects a carboxylic acid and an amine. Nevertheless, if the main reagents had been mixed without the presence of DCC, the process which would have occurred is an acid-base reaction between the acid and the amine. DCC (N,N'-dicyclohexylcarbodiimide) is an auxiliary reagent that contributes to the formation of an activated ester, a species which allows the nucleophilic acyl substitution to happen, as it is shown in the reaction mechanism in scheme 2. Apart from the amide molecule, the other main product formed in the reaction as a consequence of DCC is DCU (N,N'-dicyclohexylurea) [31].



Scheme 2. Mechanism of a nucleophilic acyl substitution between a carboxylic acid and an amine assisted by DCC.

Some experimental evidences proved the formation of pyPEG: firstly, comparing the $^1\text{H-NMR}$ spectra of reagents and products (figure 3 shows the aromatic region of 4-aminopyridine and pyPEG, which is the most clarifying in this case), variation in chemical shifts of H_α -adjacent to N in the pyridine- and H_β -not adjacent to N- indicated the formation of the product and the

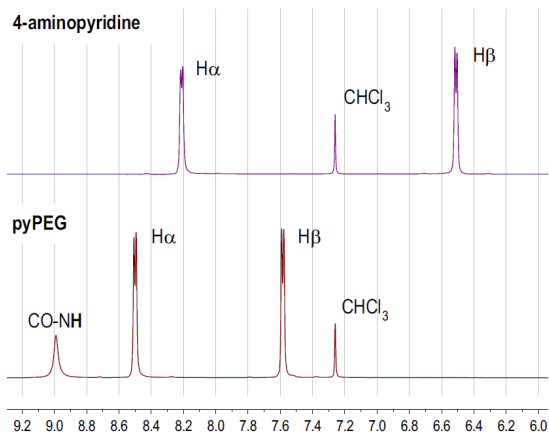


Figure 3. Aromatic region of the $^1\text{H-NMR}$ spectra of 4-aminopyridine and pyPEG in CDCl_3 .

absence of the reagent in the final substance. In addition, an indicative signal of the presence of an amide bond appeared at ca. 9 ppm in the NMR. Secondly, IR showed the carbonyl peak (1703 cm^{-1}) and also the C=N peak (1594 cm^{-1}) in the spectra of pyPEG. ESI-MS also verified the correct formation of the product with a peak at m/z 255.1347 ($[\text{M}+\text{H}]^+$ calculated m/z 255.1339).

Synthesis of $[\text{AuCl}(\text{tht})]$

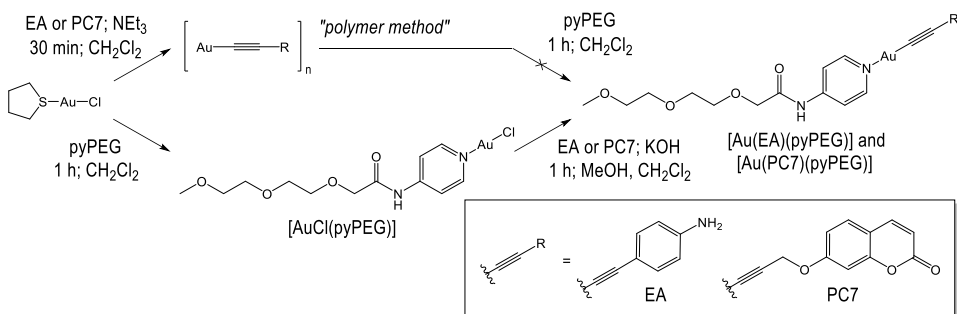
This is a routine synthesis in the research group. The color of the product is a simple indicative of its formation as tetrachloroauric acid is a yellow solid, tetrahydrothiophene is a gas and $[\text{AuCl}(\text{tht})]$ is a white solid. Besides, in the NMR spectrum of the synthesized $[\text{AuCl}(\text{tht})]$ there were two broad bands corresponding to the tht protons and no other visible signals.

Synthesis of $[\text{AuCl}(\text{pyPEG})]$, $[\text{Au}(\text{EA})(\text{pyPEG})]$ and $[\text{Au}(\text{PC7})(\text{pyPEG})]$

The first attempt to synthesize the final products, $[\text{Au}(\text{EA})(\text{pyPEG})]$ and $[\text{Au}(\text{PC7})(\text{pyPEG})]$, was incorporating the alkynyl moieties to the Au(I) centre at first, creating a polymeric $[\text{Au}(\text{C}\equiv\text{C}-\text{C}_6\text{H}_4\text{NH}_2)]_n$ structure, and then complexing the pyPEG ligand with the polymer. This reaction route, summarized in the upper part of scheme 3, had been carried out several times in the research group in similar cases of alkynyl gold(I) compounds^[10,21], although in all those cases the other ligand was a phosphane group; moreover, this method was used by Kilpin et al.^[29] to

synthesize some pyridyl gold(I) alkynyl complexes. Nevertheless, in this occasion it did not lead to successful results, as the incorporation of pyPEG in the gold(I) centres of the polymer was not produced. Kilpin et al. suggest that this method is only valid for very electron-rich pyridines – as 4-(dimethylamino)pyridine and 4-aminopyridine– in large excess because it is a Lewis acid-base reaction between Au(I) and the substituted pyridine. In our case study, the reagents and their relative proportions did not favour the formation of the desired product.

For that reason, it was decided to proceed according to an alternative method: pyPEG was coordinated to Au(I) at first and alkynyl moieties were incorporated in a second step, as it is summarized in the lower part of scheme 3.



Scheme 3. Synthetic routes tried in the synthesis of [Au(EA)(pyPEG)] and [Au(PC7)(pyPEG)]. The one in the upper part was unsuccessful and the one in the lower part lead to the desired results.

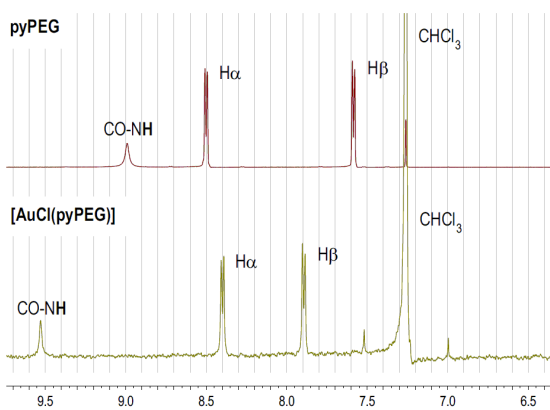


Figure 4. Aromatic region of the $^1\text{H-NMR}$ spectra of pyPEG and [AuCl(pyPEG)] in CDCl_3 .

[AuCl(pyPEG)] is the common precursor for [Au(EA)(pyPEG)] and [Au(PC7)(pyPEG)]. Its successful formation was proved by the comparison between the $^1\text{H-NMR}$ spectra of pyPEG and [AuCl(pyPEG)]: a variation in the chemical shifts was observed and no other signals were detected in the aromatic region, providing evidence of the product formation.

[Au(EA)(pyPEG)] and [Au(PC7)(pyPEG)] were successfully synthesized. Due to their lack of solubility in CDCl_3 and other solvents such as D_2O and MeOH-d_4 , $^1\text{H-NMR}$ spectra were recorded dissolving the substances in DMSO-d_6 and ACN-d_3 .

Figure 5 shows the aromatic region of spectra from [AuCl(pyPEG)], EA and [Au(EA)(pyPEG)] dissolved in deuterated acetonitrile; evidence of [Au(EA)(pyPEG)] formation was observed in these spectra. In addition, IR spectrum from [Au(EA)(pyPEG)] showed the disappearance of terminal alkynyl proton, which is an indicator of a successful coordination to gold(I) atom. ESI-MS proved the existence of [Au(EA)(pyPEG)] with the presence of a peak at m/z 568.1496 ($[\text{M}+\text{H}]^+$ calculated m/z 568.1505).

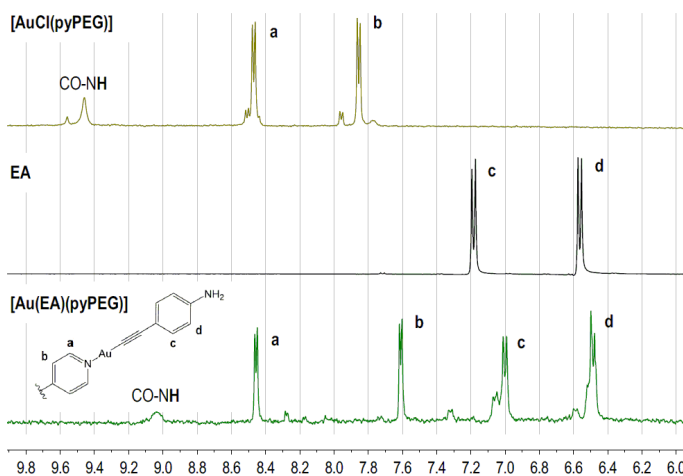


Figure 5. Aromatic region of the $^1\text{H-NMR}$ spectra from [AuCl(pyPEG)], EA and [Au(EA)(pyPEG)] dissolved in ACN-d_3 . There is a proton assignment of the signals arising from the pyridine and aniline ligands.

The NMR spectra shown in figure 5 also displayed some small signals in the aromatic region of [AuCl(pyPEG)] and [Au(EA)(pyPEG)]. This experimental fact could be explained as a degradation process of the substances in this solvent or as a symptom of aggregation: as the molecules may have more than one chemical environment when they are aggregated, there is more than one signal in the spectra associated to each proton.

All these explanations may as well be applied to [Au(PC7)(pyPEG)]. Figure 6 shows $^1\text{H-NMR}$ spectra from [AuCl(pyPEG)], PC7 and [Au(PC7)(pyPEG)], IR spectrum from

[Au(PC7)(pyPEG)] evidenced the lack of C_{sp}-H and ESI-MS proved the presence of the expected compound with a recorded peak at m/z 651.1409 ($[M+H]^+$ calculated m/z 651.1400).

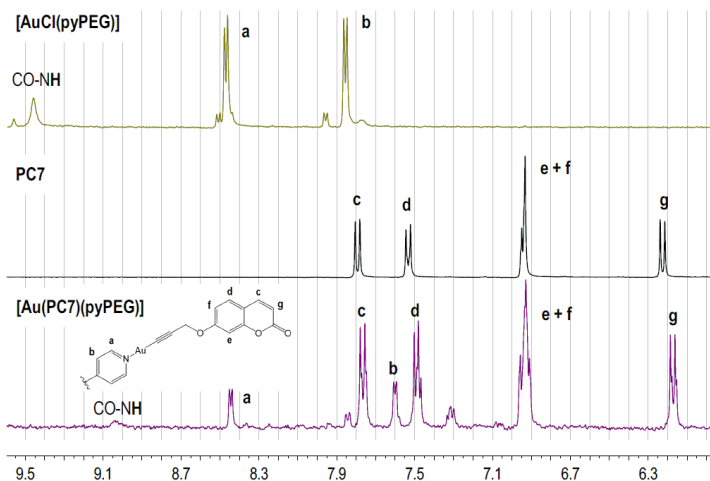


Figure 6. Aromatic region of the $^1\text{H-NMR}$ spectra from [AuCl(pyPEG)], PC7 and [Au(PC7)(pyPEG)] dissolved in ACN-d_3 . There is a proton assignment of the signals arising from the pyridine and coumarin ligands.

In order to elucidate whether the cause of the small signals in the NMR spectra from [AuCl(pyPEG)], [Au(EA)(pyPEG)] (figure 5) and [Au(PC7)(pyPEG)] (figure 6) was impurity or aggregation, they were recrystallized in THF/hexane. Unexpectedly, $^1\text{H-NMR}$ spectra from the recrystallized solid [Au(PC7)(pyPEG)] and the mother liquor showed some signals at 5-6 ppm (in figure 7 they are framed with a square).

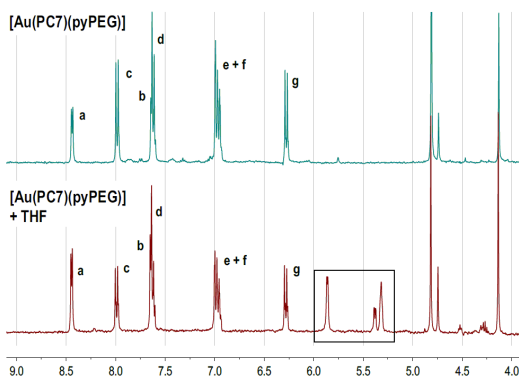


Figure 7. $^1\text{H-NMR}$ spectra from original [Au(PC7)(pyPEG)] and recrystallized [Au(PC7)(pyPEG)] in THF/hexane. They are dissolved in DMSO-d_6 . The square shows the unexpected signals.

Researching about the origin of these new signals, it was found in some recent articles [32,33] that dehydrogenative couplings reaction between coumarins and THF lead to C3 alkylation of coumarins. This reaction can occur under some conditions according to literature: the presence of a transition metal catalyst (the reported ones are copper and cobalt), an oxidation agent (the most used are organic peroxides), other additives (KI is a common additive) and heat (most reactions take place at 100 °C). In our case study, gold could have acted as a catalyst and an oxidant. Further studies have to be done in order to determine if this coupling took place.

Moreover, there were some differences between $^1\text{H-NMR}$ spectra from substances dissolved in ACN-d_3 and DMSO-d_6 , as it is observed in figures 6 and 7. They were more soluble in DMSO than in ACN and the little signals are weaker in DMSO. However, although being covered by aluminium foil, some DMSO solutions acquired a dark purple coloration several hours after being prepared and this is an indicator of the formation of $\text{Au}(0)$ nanoparticles [10], thus evidencing the degradation of the molecules. $^1\text{H-NMR}$ spectra of $[\text{Au}(\text{PC7})(\text{pyPEG})]$ DMSO solutions also supported their degradation; spectra recorded 30 min after the dissolution

process and 18 h after it are presented in figure 8. Evidence of degradation was found in the pyridine signals (around 8.2 and 8.4 ppm for H_α , around 7.5 and 7.7 ppm for H_β). A plausible explanation of the degradation is the hydrolysis of the amide bond, resulting in 4-aminopyridine–Au–PC7 in solution. On the contrary, $[\text{Au}(\text{PC7})(\text{pyPEG})]$ in ACN solutions was stable.

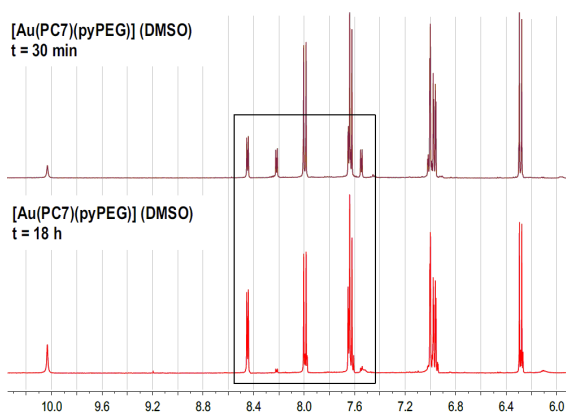


Figure 8. Aromatic region of the $^1\text{H-NMR}$ spectra from $[\text{Au}(\text{PC7})(\text{pyPEG})]$ recorded 30 min and 18 h after its dissolution in DMSO-d_6 . The changing peaks are framed.

For all those reasons, aggregation studies of $[\text{Au}(\text{PC7})(\text{pyPEG})]$ in solution were performed using ACN and ACN / H_2O mixtures as solvents. $[\text{Au}(\text{EA})(\text{pyPEG})]$ aggregation will be studied in future research projects.

6.2. PHOTOPHYSICAL CHARACTERIZATION OF [Au(PC7)(pyPEG)] SOLUTIONS

Studies on the UV-Vis absorptive and emissive properties of [Au(PC7)(pyPEG)] were carried out in ACN solutions. Spectra from pyPEG and PC7 were recorded too in order to associate each band of the absorption and emission spectra from [Au(PC7)(pyPEG)] to each chromophore group of the compound.

The electronic absorption and emission spectra were recorded for pyPEG at ca. 10^{-5} M concentration, for PC7 at ca. 10^{-4} M and for [Au(PC7)(pyPEG)] at ca. $5 \cdot 10^{-5}$ M. Absorption spectra are shown in figure 9 and quantitative values from them are summarized in table 2.

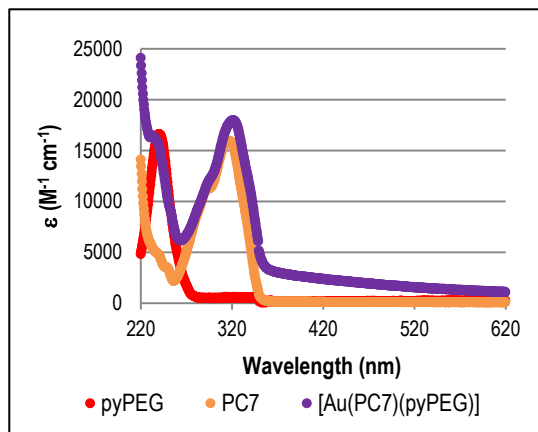


Figure 9. Absorption spectra from pyPEG, PC7 and [Au(PC7)(pyPEG)], all of them dissolved in ACN.

Emission spectra from PC7 and [Au(PC7)(pyPEG)] upon excitation at 320 nm are plotted in figure 10. They displayed a broad emission band centred at 370-410 nm caused by the coumarin $\pi-\pi^*$ fluorescent emission [20,34]. Spectrum from pyPEG showed no emission at the studied concentration. The normalized I_{emission} was notably superior in [Au(PC7)(pyPEG)] than in PC7. Excitation spectra collected at the

The electronic absorption spectrum from [Au(PC7)(pyPEG)] displayed intense bands in the range of ca. 320 nm and ca. 240 nm, which matched with the bands from PC7 and pyPEG respectively. Whereas the 320 nm band can be assigned to the $\pi-\pi^*$ transition of the 7-propargylcoumarin ligand [20,34], the 240 nm band corresponds to the $\pi-\pi^*$ transition located in the pyridine ring [25].

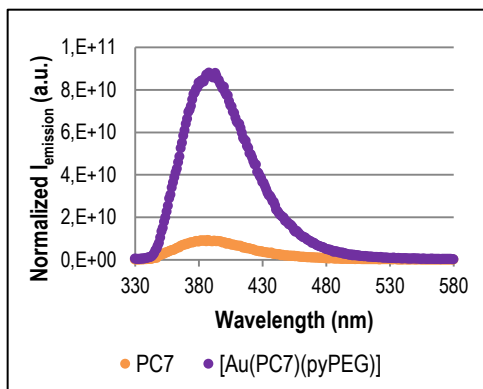


Figure 10. Normalized emission spectra from PC7 and [Au(PC7)(pyPEG)], all of them dissolved in ACN.

emission maxima reproduced absorption of the coumarin groups, which was indicative of the origin of these emission bands.

Compound	ca. c [M]	Absorption λ_{max} [nm] ($10^{-3} \epsilon$ [$\text{M}^{-1} \text{cm}^{-1}$])	Emission λ_{max} [nm] (λ_{exc} [nm])
pyPEG	$1 \cdot 10^{-5}$	240 (16.6)	- (240)
PC7	$1 \cdot 10^{-4}$	317 (16.0)	387 (320)
[Au(PC7)(pyPEG)]	$5 \cdot 10^{-5}$	234 (16.5), 321 (18.0)	388 (320)

Table 2. Absorption and emission spectral data from pyPEG, PC7 and [Au(PC7)(pyPEG)]. All compounds were dissolved in ACN.

6.3. AGGREGATION STUDIES OF [Au(PC7)(pyPEG)] SOLUTIONS

6.3.1. UV-Vis absorption and emission measurements

Aggregation studies in [Au(PC7)(pyPEG)] solutions varying its concentration

Electronic absorption and emission spectra from [Au(PC7)(pyPEG)] solutions were recorded varying its concentration between ca. $5 \cdot 10^{-7}$ M and ca. $1 \cdot 10^{-4}$ M. The studies were performed in DMSO/H₂O, ACN and ACN/H₂O systems; however, since the solute is not stable in DMSO, the results of the experiments performed in DMSO/H₂O will not be discussed herein.

Regarding to studies in pure ACN, absorption spectra from solutions between $1 \cdot 10^{-4}$ M and $2.5 \cdot 10^{-6}$ M displayed the intense band from the coumarin unit (figure 11, upper left); its maximum absorbance value was placed at 319-322 nm. At lower concentrations, the band was not clearly defined. The pyridine band at 237-340 nm was clearly distinguished in the spectra from most concentrated solutions.

Furthermore, there was a notable baseline increase in the absorption spectra from solutions at $5 \cdot 10^{-5}$ M and upwards; this is a consequence of light scattering due to precipitation/aggregation phenomena [11]. Also, when representing absorbance at 320 nm against concentration, a linear behaviour was observed (figure 11, upper right).

Emission spectra from [Au(PC7)(pyPEG)] solutions in ACN ($\lambda_{\text{exc}} = 320$ nm) presented the same profile between ca. $1 \cdot 10^{-6}$ M and $1 \cdot 10^{-4}$ M concentration (figure 11, lower left). Only one emission band with its maximum placed at 386-392 nm was observed in all cases. Intensity of emission at 392 nm against concentration plot displayed linearity until $1 \cdot 10^{-5}$ M and a loss of linear behaviour was observed upwards (figure 11, lower right); this loss of linearity was

associated to aggregation. Taking these details into account, an aggregation critical concentration was detected between $1 \cdot 10^{-5}$ M and $5 \cdot 10^{-5}$ M. More emission measurements need to be carried out to know the exact value of this aggregation critical concentration.

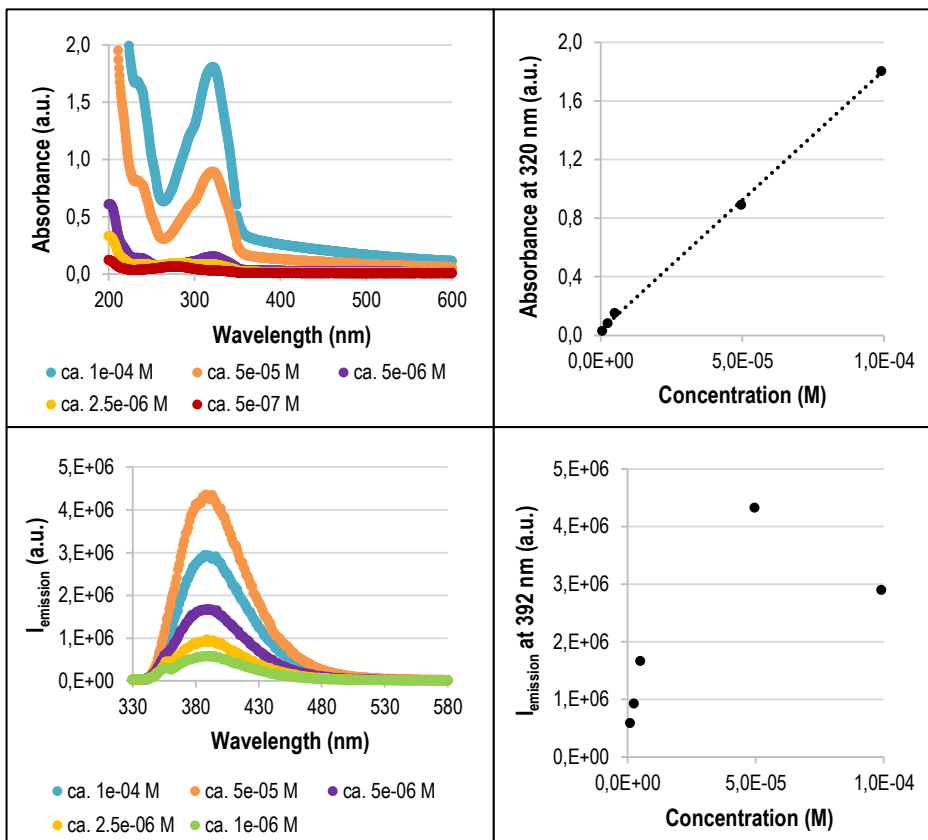


Figure 11. Some data of absorption and emission spectra from [Au(PC7)(pyPEG)] solutions in ACN.

Regarding to studies in ACN 75% / H₂O 25%, absorption spectra from solutions at ca. $2.5 \cdot 10^{-6}$ M - $1 \cdot 10^{-4}$ M concentrations showed coumarin bands with maximum absorbance at 321-325 nm, slightly red-shifted compared to ACN solutions, and pyridine bands at 243-244 nm (figure 12, upper left). The same aspects related to baseline and linearity of absorbance against concentration (figure 12, upper right) may be applied to these solutions.

Emission spectra from [Au(PC7)(pyPEG)] solutions in ACN 75% / H₂O 25% ($\lambda_{exc} = 320$ nm) presented the same profile at ca. $5 \cdot 10^{-7}$ M - $1 \cdot 10^{-4}$ M concentrations (figure 12, lower left). They

displayed an intense emissive band at 390-396 nm, also slightly red-shifted with respect to ACN equivalent solutions. In addition, a less intense band at 480-485 nm was visually detected in the spectra. It corresponds to a 0-0 phosphorescent emission of the coumarin^[34] and its existence is associated to a stronger heavy atom effect of Au(I), therefore to higher supramolecular interactions in which gold is involved and consequently to a larger aggregation phenomenon^[35]. The intensity of emission against concentration plots showed linearity at low concentrations until $1 \cdot 10^{-5}$ M and a loss of the linear behaviour was observed in higher concentrations (figure 12, lower right). All these evidences led to state that aggregation in [Au(PC7)(pyPEG)] solutions in ACN 75% / H₂O 25% exists at concentrations of ca. $5 \cdot 10^{-6}$ M –which is the approximate value of the aggregation critical concentration– and upwards.

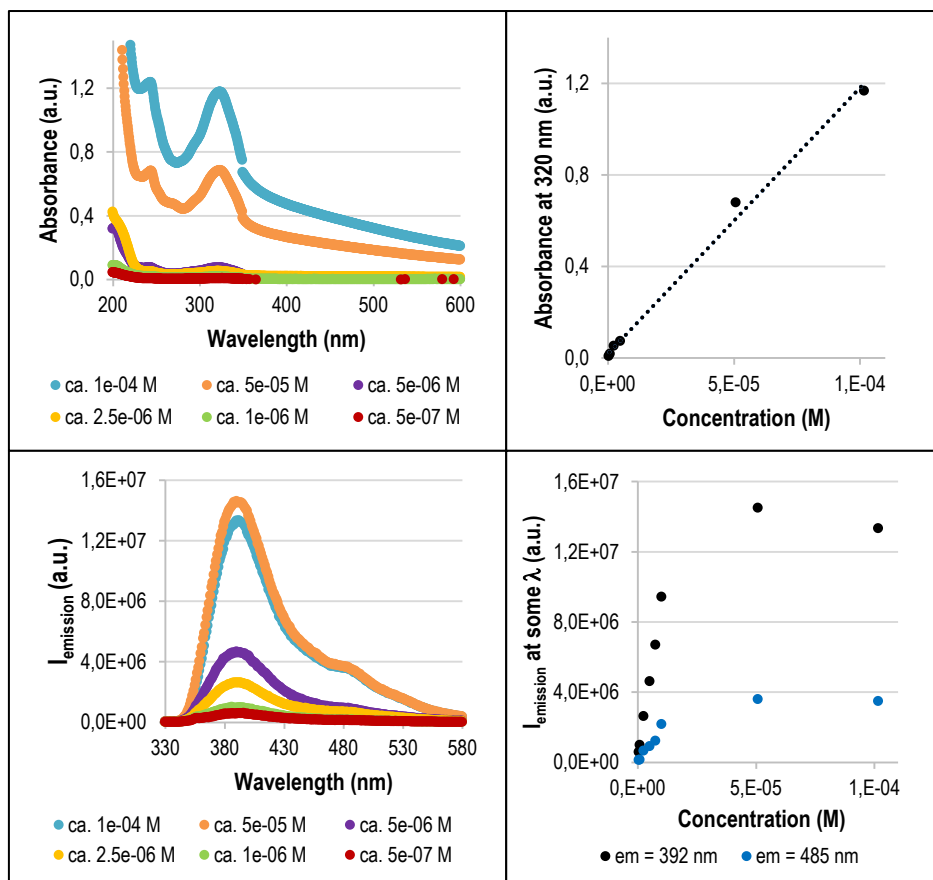


Figure 12. Some data of absorption and emission spectra from [Au(PC7)(pyPEG)] solutions in ACN 75% / H₂O 25%.

Comparing equivalent solutions in different solvent systems (figures 11 and 12), the global tendency is that the presence of water leads to higher dispersion of the baseline, lower absorbance of the absorption bands and greater intensity of the emission bands.

Aggregation studies in [Au(PC7)(pyPEG)] solutions varying the solvent composition

UV-Vis absorption and emission measurements were applied to sets of [Au(PC7)(pyPEG)] solutions with a constant concentration of 10^{-4} M or 10^{-5} M varying the percentage of H₂O in the solvent system. Figure 13 summarizes the most significant information from 10^{-4} M solutions.

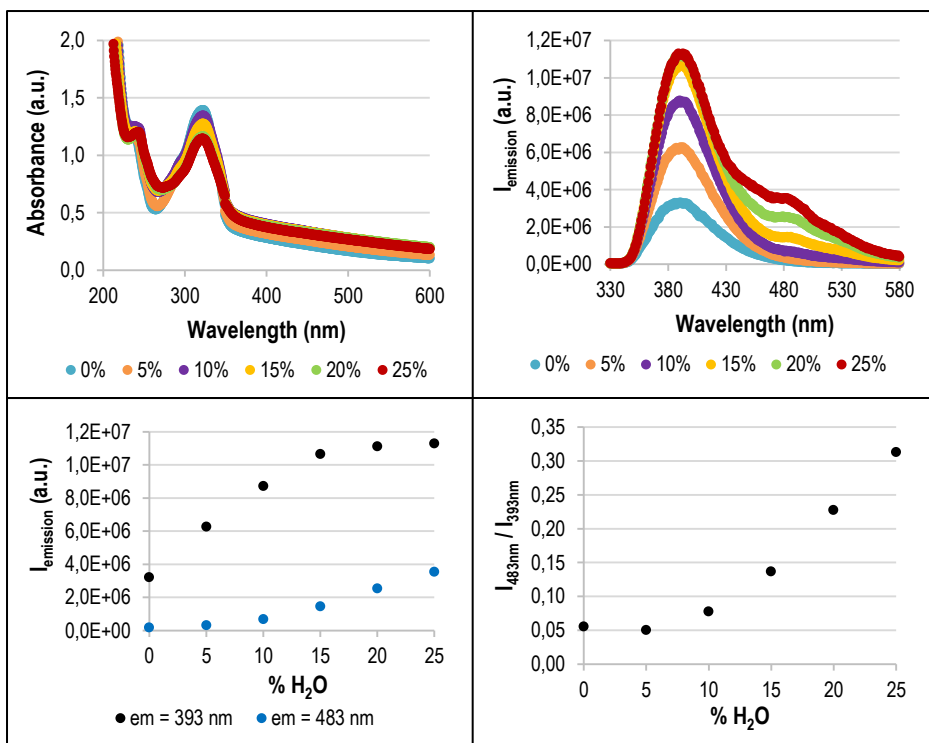


Figure 13. Some data of absorption and emission spectra from 10^{-4} M [Au(PC7)(pyPEG)] solutions in ACN / H₂O systems (0-25% H₂O).

Absorption spectra showed that higher H₂O proportions may be associated with more significant baseline dispersion and consequently larger aggregation/precipitation. Absorption bands had no wavelength shifting when varying the relative amount of water: the absorbance

maximum was always placed at 319-323 nm. All these explanations can be referred to both 10^{-4} M (figure 13, upper left) and 10^{-5} M sets of measures.

Besides, emission spectra ($\lambda_{exc} = 320$ nm) changed gradually when increasing the water proportion. Whereas in ACN phosphorescence bands did not exist, in ACN / H₂O they became visible: in 10^{-4} M solutions it was possible to distinguish visually the phosphorescence band at 10% of H₂O and upwards (figure 13, upper right); in 10^{-5} M solutions this limit was at 15%.

In addition, considering the intensity against % of H₂O plots, a loss of linearity at 10-15% in 10^{-4} M solutions was detected (figure 13, lower left). In the case of 10^{-5} M solutions, no linearity loss was observed. Finally, the phosphorescence / fluorescence emission ratio in 10^{-4} M solutions was constant at 0-5% of water and increased notably as the relative content of water in the solvent became larger (figure 13, lower right); this is another evidence of aggregation.

General statements about aggregation studies with UV-Vis measurements

Taking into consideration the observations described in the previous paragraphs and figures, the aggregation studies of [Au(PC7)(pyPEG)] solutions lead to the following statements:

- Aggregation and concentration are directly related, when one increases the other too. There are certain concentration values, different in each solvent system, which can be considered aggregation critical concentrations. This experimental evidence is coherent with the theoretical conception of aggregation as a chemical equilibrium: when the concentration is higher, the aggregation equilibrium is shifted to the existence of more self-organized structures.
- The presence of water in the solvent leads to a greater aggregation and causes lower aggregation critical concentrations. A molecular explanation of this trend would be that due to the lack of solubility of the compound in water, in an aqueous solution its molecules tend to form aggregates orienting themselves to keep the less soluble parts in the interior of these aggregates in order to avoid the solvent. Thus, in an ACN / H₂O solution, a higher content of water causes a larger aggregation.
- Some clear indicators of aggregation in [Au(PC7)(pyPEG)] solutions using UV-Vis measurements are a modification of the baseline in absorption spectra, a loss of linearity in emission intensity against concentration plots and an the presence of phosphorescence bands at ca. 480-485 nm.

6.3.2. NMR spectroscopy

Even though aggregation studies of [Au(PC7)(pyPEG)] solutions by means of NMR spectroscopy were planned to be done in this research project, the other experimental parts made it impossible to perform a deep study by means of 1D and 2D NMR experiments that can provide significant information about which parts of the molecule are directly involved in the aggregation process. They will be carried out after this TFG project.

6.3.3. SAXS

X-ray scattering techniques are a set of analytical techniques based on measuring the scattered intensity of an X-ray beam interacting with a sample. Concretely, small angle X-ray scattering (SAXS) is a technique that reveals information about structural features of substances in the nanometric and colloidal scales [36]. One of the most significant advantages of this technique is that the sample does not necessarily have to be a crystalline structure.

As X-ray wavelength is extremely small compared with dimensions of the substance, the particles that interact with X-rays are electrons; they resonate with the frequency of the radiation and their secondary emissions interfere with each other, causing a scattering phenomenon. Consequently, small angle scattering is observed when there are electron density inhomogeneities in the sample, which can have a size from a few Angstroms to a few microns. The data collected in the scattering process (which is a series of scattered intensity vs 2θ paired data) can be treated with Fourier transformations and other mathematical operations in order to deduce the size, shape and electron density distribution of the structures present in the sample [37].

SAXS measures have to be performed with synchrotron radiation. This type of radiation is characterized by having a very high intensity, a very good intrinsic collimation and a pulsed emission [37]. For this reason, SAXS measures of this work were performed on the NCD (Non Crystalline Diffraction) beamline at the Alba Synchrotron. [Au(PC7)(pyPEG)] solutions with a molar concentration of ca. $1 \cdot 10^{-4}$ M and $1 \cdot 10^{-5}$ M dissolved in ACN / H₂O mixtures were analysed and their low-resolution structures were reconstructed ab initio from the scattering patterns using the *DAMMIN* program [30]. Some representative experiment results are shown in table 3.

All the SAXS structures presented herein are the average result of 10 scattering measurements. The spheres that integrate the represented aggregates are only representations made by the program; for complex particle shapes, it approximates the particle as a cumulus of small, closely packed spheres.

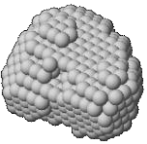
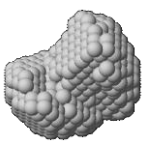
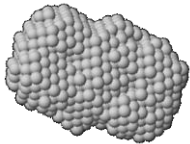
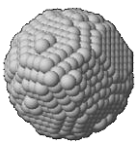
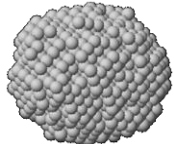
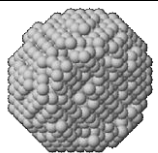
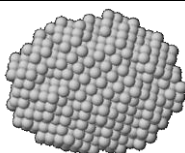
Sample	Size (Å)	Structure	Sample	Size (Å)	Structure
0% H ₂ O, 1·10 ⁻⁴ M	95		0% H ₂ O, 1·10 ⁻⁵ M	No aggregates were found	
10% H ₂ O, 1·10 ⁻⁴ M	147		10% H ₂ O, 1·10 ⁻⁵ M	322	
25% H ₂ O, 1·10 ⁻⁴ M	142		25% H ₂ O, 1·10 ⁻⁵ M	290	
75% H ₂ O, 1·10 ⁻⁴ M	225		75% H ₂ O, 1·10 ⁻⁵ M	380	

Table 3. DAMMIN low-resolution structures and sizes reconstructed from SAXS patterns.

The absence of aggregation in the 10⁻⁵ M sample in pure ACN and the existence of it in the 10⁻⁴ M sample are coherent with what has been discussed in the absorption and emission measurements section: the aggregation critical concentration in ACN has an approximate value between 10⁻⁵ M and 10⁻⁴ M.

As it can be seen in table 3, one general tendency is that aggregates had a bigger dimension in 10⁻⁵ M samples than in 10⁻⁴ M samples. A possible explanation to this experimental evidence is that the lower the solute concentration is, less packed are the molecules and therefore the aggregates have a lower density and a bigger size. Another

general behaviour is that aggregates were bigger in solvent systems with a higher proportion of water; again, this tendency is coherent with absorption and emission results, as it was proved that aggregation was stronger as more aqueous is the solvent.

However, despite the fact that variation of solvents and concentrations caused different sizes in the aggregates, all of them presented a spherical or ellipsoidal shape with no significant differences among them.

6.3.4. Optical microscopy

Observing supramolecular aggregates with an optical microscope can give information about their organization in the mesoscopic scale, especially using polarized light. Using two crossed polarizing filters, the anisotropy of organized structures gives rise to their visibility, whereas isotropic substances remain dark.

Figure 14 is a photograph taken in the observation of an $[\text{Au}(\text{PC7})(\text{pyPEG})]$ 2-day-old dried sample from an ACN 75% / H_2O 25% solution. It is particularly interesting because on the one hand it shows the existence of micrometric short fibres in solution but on the other hand there are some little spheres in the surface of the fibres and in some areas they agglomerate with each other, leading to the formation of larger

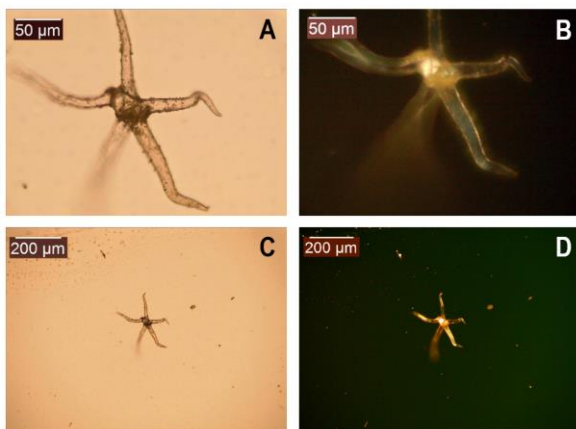


Figure 14. Optical microscopy images of a dried $[\text{Au}(\text{PC7})(\text{pyPEG})]$ solution at $5 \cdot 10^{-6}$ M concentration in an ACN 75% / H_2O 25% solvent system. B and D were taken by observation of the sample between crossed polarizers.

structures which result in short fibres in this case. Thus, figure 14 is an experimental evidence of the existence of different levels of organization and therefore different stages of aggregation in the samples.

Moreover, other shapes and morphologies were observed in $[\text{Au}(\text{PC7})(\text{pyPEG})]$ solutions in ACN 75% / H_2O 25%; some of them are shown in figure 15. However, self-organization was

observed in all samples dissolved in this solvent system ($5 \cdot 10^{-7}$ M to $1 \cdot 10^{-4}$ M). The supramolecular architectures that were seen in them include vesicles and short fibres. These images evidence the formation of mesoscopic supramolecular aggregates.

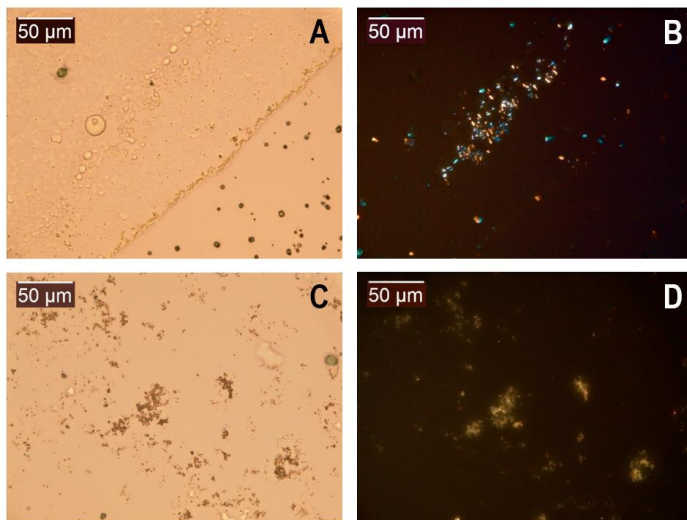


Figure 15. Optical microscopy images of some dried $[Au(PC7)(pyPEG)]$ solutions in ACN 75% / H_2O 25%. A and B are from a $1 \cdot 10^{-4}$ M sample; C and D are from a $5 \cdot 10^{-5}$ M sample. B and D were taken by observation of the sample between crossed polarizers.

7. CONCLUSIONS

N-(4-pyridyl)2-[2-(2-methoxyethoxy)ethoxy]acetic acid amide (pyPEG) can be complexed to gold to constitute Au(I) alkynyl organometallic compounds containing pyridine as the second coordination position by choosing the adequate experimental methodology. The polymer method, using alkynyl gold(I) polymers as precursors of pyPEG alkynyl gold(I) complexes, does not lead to the desired synthesis; alternatively, incorporating the pyPEG ligand prior to the alkynyl moiety lead the expected compounds to be synthesized.

[Au(PC7)(pyPEG)] is stable and forms aggregates in ACN and ACN/H₂O solutions. Nevertheless, it is not stable in DMSO neither in THF.

Some indicators relative to UV-Vis absorption and emission measurements which provide an experimental evidence of aggregation in [Au(PC7)(pyPEG)] solutions are a baseline dispersion effect in absorption spectra, loss of linearity in the emission intensity against concentration plot and the presence of phosphorescence bands from the coumarin moiety at ca. 480-485 nm.

1D and 2D NMR experiments will be a decisive tool to study which moieties of the molecule are directly involved in the aggregation process. This study is expected to be performed after this TFG work.

A larger concentration of the solute in the studied systems implies an increased aggregation. There are some concrete concentration values that suppose a change in aggregation: whereas at lower concentrations there is no significative self-organization of the molecules, higher concentrations lead to the formation of aggregates. Moreover, a larger relative content of water in the solvent increases the aggregation rate and causes lower aggregation critical concentrations.

Aggregation in [Au(PC7)(pyPEG)] solutions is experimentally evidenced by SAXS results and optical microscopy. The aggregates present spherical and ellipsoidal shapes in the nanoscale and form complex architectures with different levels of organization, leading to different morphologies, such as vesicles and short fibres.

8. REFERENCES AND NOTES

- [1] Schmidbaur, H. The fascinating implications of new results in gold chemistry. *Gold Bull.* **1990**, *23*(1), 11-21.
- [2] Pyykkö, P.; Zhao, Y. The ab initio calculations for the dimer chloro(phosphine)gold [ClAuPH₃]₂ with relativistic pseudopotential. Is the aurophile attraction a correlation effect? *Angew. Chem.* **1991**, *103*(5), 622-623.
- [3] Schmidbaur, H. The Aurophilicity Phenomenon: A Decade of Experimental Findings, Theoretical Concepts and Emerging Applications. *Gold Bull.* **2000**, *33*(1), 3-10.
- [4] Ka-Wah Hau, F.; Wing-Wah Yam, V. Synthesis and cation-binding studies of gold(I) complexes bearing oligoether isocyanide ligands with ester and amide as linkers. *Dalton Trans.* **2016**, *45*, 300-306.
- [5] You, L.; Zha, D.; Anslyn, E. V. Recent Advances in Supramolecular Analytical Chemistry Using Optical Sensing. *Chem. Rev.* **2015**, *115*(15), 7840-7892.
- [6] Jürgens, S.; Casini, A. Mechanistic Insights into Gold Organometallic Compounds and their Biomedical Applications. *Chimia International Journal for Chemistry.* **2017**, *71*(3), 92-101.
- [7] Song, T.; Xiao, S.; Yao, D.; Huang, F.; Hu, M.; Liang, H. An Efficient DNA-Fueled Molecular Machine for the Discrimination of Single-Base Changes. *Adv.Mater.* **2014**, *26*(35), 6181-6185.
- [8] Gavara, R.; Llorca, J.; Lima, J. C.; Rodríguez, L. A luminescent hydrogel based on a new Au(I) complex. *Chem. Commun.* **2013**, *49*, 72-74.
- [9] Tam, A. Y.-Y.; Yam, V. W.-W. Recent advances in metallogels. *Chem. Soc. Rev.* **2013**, *42*, 1540-1567.
- [10] Aguiló, E.; Gavara, R.; Lima, J. C.; Llorca, J.; Rodríguez, L. From Au(I) organometallic hydrogels to well-defined Au(0) nanoparticles. *J. Mater. Chem. C.* **2013**, *1*, 5538-5547.
- [11] Moro, A. J.; Rome, B.; Aguiló, E.; Arcau, J.; Puttreddy, R.; Rissanen, K.; Lima, J. C.; Rodríguez, L. A coumarin based gold(I)-alkynyl complex: a new class of supramolecular hydrogelators. *Org. Biomol. Chem.* **2015**, *13*, 2026-2033.
- [12] Gavara, R.; Aguiló, E.; Fonseca Guerra, C.; Rodríguez, L.; Lima, J. C. Thermodynamic Aspects of Aurophilic Hydrogelators. *Inorg. Chem.* **2015**, *54*, 5195-5203.
- [13] Aguiló, E.; Gavara, R.; Baucells, C.; Guitart, M.; Lima, J. C.; Llorca, J.; Rodríguez, L. Tuning supramolecular aurophilic structures: the effect of counterion, positive charge and solvent. *Dalton Trans.* **2016**, *45*, 7528-7539.
- [14] Pinto, A.; Svahn, N.; Lima, J. C.; Rodríguez, L. Aggregation induced emission of gold(I) complexes in water or water mixtures. *Dalton Trans.* **2017**, *46*, 11125-11139.
- [15] Schröder, T.; Geisler, T.; Walhorn, V.; Schnatwinkel, B.; Anselmetti, D.; Mattay, J. Single-molecule force spectroscopy of supramolecular heterodimeric capsules. *Phys. Chem. Chem. Phys.* **2010**, *12*, 10981-10987.
- [16] Hua, F.; Yang, X.; Gong, B.; Ruckenstein, E. Preparation of oligoamide-ended poly(ethylene glycol) and hydrogen-bonding-assisted formation of aggregates and nanoscale fibers. *J. Polym. Sci. A.* **2005**, *43*, 1119-1128.
- [17] Lin, Y.; Yin, J.; Yuan, J.; Hu, M.; Li, Z.; Yu, G.; Liu, S. Synthesis, Characterization, and Properties of Binuclear Gold (I) Phosphine Alkynyl Complexes. *Organometallics.* **2010**, *29*, 2808-2814.
- [18] Najmul Islam, S.; Sil, A.; Patra, S. K. Achieving yellow emission by varying the donor/acceptor units in rod-shaped fluorenyl-alkynyl based π -conjugated oligomers and their binuclear gold(I) alkynyl complexes. *Dalton Trans.* **2017**, *46*, 5918-5929.
- [19] Lima, J. C.; Rodríguez, L. Supramolecular Gold Metallogelators: The Key Role of Metallophilic Interactions. *Inorganics.* **2015**, *3*(1), 1-18.
- [20] Arcau, J.; Andermark, V.; Aguiló, E.; Gandioso, A.; Moro, A.; Cetina, M.; Lima, J. C.; Rissanen, K.; Ott, I.; Rodríguez, L. Luminescent alkynyl-gold(I) coumarin derivatives and their biological activity. *Dalton Trans.* **2014**, *43*, 4426-4436.

- [21] Aguiló, E.; Moro, A. J.; Gavara, R.; Alfonso, I.; Pérez, Y.; Zaccaria, F.; Fonseca Guerra, C.; Malfois, M.; Baucells, C.; Ferrer, M.; Lima, J. C.; Rodríguez, L. Reversible Self-Assembly of Water-Soluble Gold(I) Complexes. *Inorg. Chem.* **2018**, *57*, 1017-1028.
- [22] Seixas de Melo, J. S.; Becker, R. S.; Maçanita, A. L. Photophysical Behavior of Coumarins as a Function of Substitution and Solvent: Experimental Evidence for the Existence of a Lowest Lying (n, π^*) State. *J. Phys. Chem.* **1994**, *98*, 6054-6058.
- [23] Gandioso, A.; Bresoli-Obach, R.; Nin-Hill, A.; Bosch, M.; Palau, M.; Galindo, A.; Contreras, S.; Rovira, A.; Rovira, C.; Nonell, S.; Marchán, V. Redesigning the Coumarin Scaffold into Small Bright Fluorophores with Far-Red to Near-Infrared Emission and Large Stokes Shifts Useful for Cell Imaging. *J. Org. Chem.* **2018**, *83*, 1185-1195.
- [24] Mullice, L. A.; Thorp-Greenwood, F. L.; Laye, R. H.; Coogan, M. P.; Kariuki, B. M.; Pope, S. J. A. The coordination chemistry of fluorescent pyridinyl- and quinolonyl-phthalimide ligands with the $[\text{Au}^{\text{I}}\text{PPh}_3]$ cationic unit. *Dalton Trans.* **2009**, *0*, 6836-6842.
- [25] Fernández, E. J.; Laguna, A.; López-de-Luzuriaga, J. M.; Monge, M.; Montiel, M.; Olmos, M. E.; Pérez, J.; Rodríguez-Castillo, M. Pyridine Gold Complexes. An Emerging Class of Luminescent Materials. *Gold Bull.* **2007**, *40*(3), 172-183.
- [26] Aliprandi, A.; Mauro, M.; De Cola, L. Controlling and imaging biomimetic self-assembly. *Nat. Chem.* **2016**, *8*, 10-15.
- [27] Carrara, S.; Aliprandi, A.; Hogan, C. F.; De Cola, L. Aggregation-Induced Electrochemiluminescence of Platinum(II) Complexes. *J. Am. Chem. Soc.* **2017**, *139*(41), 14605-14610.
- [28] Usón, R.; Laguna, A.; Laguna, M.; Briggs, D. A.; Murray, H. H.; Fackler, J. P. Tetrahydrothiophene gold(I) or gold(III) complexes. *Inorg. Synth.* **1989**, *26*, 322.
- [29] Kilpin, K. J.; Horvath, R.; Jameson, G. B.; Telfer, S. G.; Gordon, K. C.; Crowley, J. D. Pyridyl Gold(I) Alkynyls: A Synthetic, Structural, Spectroscopic, and Computational Study. *Organometallics.* **2010**, *29*, 6186-6195.
- [30] Svergun, D. I. Restoring Low Resolution Structure of Biological Macromolecules from Solution Scattering Using Simulated Annealing. *Biophys. J.* **1999**, *76*, 2879.
- [31] Bruice, P. Y. (2007). *Organic chemistry*. 5th ed. Upper Saddle River, New Jersey (USA): Pearson Prentice Hall.
- [32] Wang, C.; Mi, X.; Li, Q.; Li, Y.; Huang, M.; Zhang, J.; Wu, Y.; Wu, Y. Copper-catalyzed cross-dehydrogenative-coupling (CDC) of coumarins with cyclic ethers and cycloalkane. *Tetrahedron.* **2015**, *71*, 6689-6693.
- [33] Dian, L.; Zhao, H.; Zhang-Negrerie, D.; Du, Y. Cobalt-Catalyzed Twofold Direct $\text{C}(\text{sp}^2)\text{-C}(\text{sp}^2)$ Bond Coupling: Regioselective C-3 Alkylation of Coumarins with (Cyclo)alkyl Ethers. *Adv. Synth. Catal.* **2016**, *358*, 2422-2426.
- [34] Jacquemin, D.; Perpète, E. A.; Scalmani, G.; Frisch, M. J.; Assfeld, X.; Ciofini, I.; Adamo, C.. Time-dependent density functional theory investigation of the absorption, fluorescence and phosphorescence spectra or solvated coumarins. *J. Chem. Phys.* **2006**, *125*, 164324(1-11).
- [35] Rodríguez, L.; Ferrer, M.; Crehuet, R.; Anglada, J.; Lima, J. C. Correlation between Photophysical Parameters and Gold-Gold Distances in Gold(I) (4-Pyridyl)ethynyl Complexes. *Inorg. Chem.* **2012**, *51*, 7636-7641.
- [36] Alba Synchrotron. Beamline BL11 – NCD-Sweet: beamline information. Retrieved from <https://www.cells.es/en/beamlines/bl11-ncd> [consulted in 04/06/2018].
- [37] Glatter, O.; Kratky, O. (Ed.). (1982). *Small Angle X-ray Scattering*. New York, USA: Academic Press.

9. ACRONYMS

Reagents and products

DCC – N,N'-dicyclohexylcarbodiimide

DCU – N,N'-dicyclohexylurea

EA – 4-ethynylaniline

PC7 – 7-propargylcoumarin

PEG – polyethylene glycol

pyPEG – N-(4-pyridyl)2-[2-(2-methoxyethoxy)ethoxy]acetic acid amide

tht – tetrahydrothiophene

Solvents and solutions

ACN – acetonitrile

AcOEt – ethyl acetate

DMSO – dimethyl sulfoxide

EtOH – ethanol

MeOH – methanol

p.a. – purity for analysis

THF – tetrahydrofuran

Techniques

ESI-MS – electrospray ionization mass spectrometry

IR – infrared

NCD – non crystalline diffraction

NMR – nuclear magnetic resonance

SAXS – small angle X-ray scattering

UV-Vis – ultraviolet-visible

TLC – thin layer chromatography

Nuclear magnetic resonance

br. – broad

d – doublet

m – multiplet

s – singlet

